46th AIAA Aerospace Sciences Meeting and Exhibit
7 - 10 January 2008, Reno, Nevada

AIAA 2008-576

Experimental Study of Cryogenic Cavitation Using Fluoroketone

Jonas P. R. Gustavsson*, Kyle Denning† and Corin Segal‡
Department of Mechanical and Aerospace Engineering,
University of Florida, Gainesville, FL 32611

Cavitation under simulated cryogenic conditions was studied on a NACA0015 hydrofoil in a watertunnel filled with the perfluorinated ketone 2-trifluoromethyl-1,1,1,2,4,4,5,5,5-nonafluoro-3-pentanone. Through pressure measurements on the hydrofoil, flash high-speed photography and laser-induced fluorescence in the fluoroketone medium, the extent of cavitation and the characteristic frequencies of its oscillation were studied under varying speeds and angle of attack. While St_c=0.56 oscillations were found for a wide range of conditions, these were attributed to effects of dissolved gas. For properly degassed fluoroketone, Mode I-II cavitation transition was observed to occur in a generally similar manner to in water. The size of the formed bubbles was found to be significantly smaller than in water tests under similar conditions.

Nomenclature

α	=	angle of attack
C_P	=	pressure coefficient
$C_{P,l}$	=	specific heat of liquid phase
c	=	chord length
ΔH_{vap}	=	heat of vaporization
ΔT	=	local temperature depression due to thermodynamic effect
f	=	frequency
k	=	thermal conductivity
μ	=	dynamic viscosity, $\rho\nu$
ν	=	kinematic viscosity
P	=	static pressure
P_0	=	stagnation pressure
P_∞	=	freestream static pressure in testsection
P_v	=	vapor pressure
Pr	=	Prandtl number of fluid, $C_{P,l}\mu/k$
Re	=	Reynolds number, $U_\infty c/\nu$
ρ	=	density
ρ_l	=	density of liquid phase
ρ_v	=	density of vapor phase
σ	=	cavitation number, $(P-P_v)/(\frac{1}{2}\rho U_\infty^2)$
St_c	=	Strouhal number based on chord length, fc/U_∞
U_∞	=	freestream velocity at centerline in testsection

* Postdoctoral Associate, Mechanical and Aerospace Engineering, MAE-A 231, PO Box 116250, University of Florida, Gainesville, FL 32611, Member AIAA
† Undergraduate Assistant, Mechanical and Aerospace Engineering, MAE-A 231, PO Box 116250, University of Florida, Gainesville, FL 32611, Student Member AIAA
‡ Associate Professor, Mechanical and Aerospace Engineering, MAE-A 231, PO Box 116250, University of Florida, Gainesville, FL 32611, Associate Fellow AIAA

I. Introduction

A. Fundamentals

CAVITATION is a major concern in the design of turbopumps due to the performance degradation, vibrations, flow unsteadiness and erosion damage that it can create. The primary parameter for determining the presence and quality of cavitation is the cavitation number σ:

$$\sigma = \frac{P_\infty - P_v}{\frac{1}{2}\rho U_\infty^2} \tag{1}$$

As a first approximation, cavitation, i. e. the formation of vapor bubbles due to a drop in local static pressure, occurs when the cavitation number reaches $-C_P$, i. e. when the local static pressure is equal to the fluid vapor saturation pressure. Since the saturation vapor pressure is a function of temperature, a flow or evaporation-induced change in the local temperature greatly complicates the prediction of cavitation onset. For water near ambient conditions, the temperature change is often negligible, but for other materials the localized cooling of the liquid phase in the vicinity of a forming vapor bubble, referred to as the thermodynamic effect, must be considered. The temperature decrease can be estimated as $\Delta T = B\Delta T^*$:

$$\Delta T^* = \frac{\Delta H_{vap}}{C_{p,l}} \frac{\rho_v}{\rho_l} \tag{2}$$

A scaling of the dimensionless B-factor as $B = Re^{0.2}Pr^{0.7}$ has been suggested by Franc et al.[1] A discussion of different temperature depression models and experimental data for different geometries and fluids, illustrating the difficulty of finding a valid general correlation, has been given by Billet et al.[2]

B. Tests in Water

For practical reasons, a majority of cavitation tests have been carried out in water.[3] It has been found that dissolved gas in the liquid may have a substantial effect on incipient cavitation through facilitating the growth of bubbles starting on a gas kernel through lowering the pressure threshold due to surface tension that needs to be overcome. Dissolved gas also appears to smoothen the bubble collapse, potentially decreasing the peak pressure as the bubble rebounds, weakening the impinging jet that is suspected to cause cavitation damage.[4]

The NACA0015 hydrofoil is one of the most studied geometries, establishing a substantial database for cavitation behavior at varying cavitation numbers. The pressure oscillations are characterized using a Strouhal number based on chord length:

$$St_c = \frac{U_\infty f}{c} \tag{3}$$

At low cavitation numbers, corresponding to Mode I cloud cavitation, the spectrum is dominated by a sharp peak in the range $0.1 < St_c < 0.2$. At higher cavitation numbers, corresponding to Mode II the literature shows a larger range of behaviors, but generally there is a second peak at higher Strouhal numbers. Kjeldsen et al[5] found Strouhal numbers in this regime increasing with increasing cavitation numbers from $St_c = 0.45$ at $\sigma = 1$ to $St_c = 0.6$ at $\sigma = 1.3$, both at $\alpha = 7°$. It has been suggested that in this regime, the Strouhal number based on cavity length may remain constant, $St_{Lcav} \approx 0.3$.[5]

C. Tests with Substantial Thermodynamic Effect

Due to its large density ratio, ρ_l/ρ_v, water exhibits a limited thermodynamic effect, i. e. low ΔT^*, at ambient conditions and this is difficult to increase appreciably due to the inaccessibility of the water critical point. On the other hand, liquid hydrogen, which goes from subcritical to supercritical conditions as it passes through the low pressure fuel turbopump in the Space Shuttle, exhibits a significant thermodynamic effect. This leads to a reduction in the amount of vapor generated at a certain σ, facilitating the restart of a partially vapor-filled turbopump and reducing the demand for a chilldown system in rocket applications.[6] The flow is challenging to simulate because

instead of, as in water cavitation, having discrete vapor and liquid regions separated by a simple surface, it tends to contain extended regions of two-phase, frothy mixtures. Due to their great compliance, the local speed of sound is so low, often a few m/s, that compressible effects, such as choking and shock waves, become important. This implies that experimental data for CFD code validation under conditions with strong thermodynamic effect are needed.

D. Present study

To allow us to study the impact that the thermodynamic effect has on cavitation without the risks and thermal management problems of having a large-scale flow facility filled with liquid hydrogen, we have chosen to investigate the flow using a fluoroketone that is liquid under ambient conditions, inflammable and has a critical point of 442 K, 1.87 MPa. In addition to these features, the fluoroketone also exhibits strong fluorescence with an absorption in the near UV, maximum at 305 nm, and emission in the blue region of the visible spectrum.[7] This allows us to use laser-induced fluorescence to study the extent of the cavitating region non-invasively using a 351 nm laser for excitation.

II. Experimental Setup

A. Watertunnel

A watertunnel with 102x102 mm cross section testsection was constructed for these experiments and filled with the perfluorinated ketone 2-trifluoromethyl-1,1,1,2,4,4,5,5,5-nonafluoro-3-pentanone. The tunnel shown in Figure 1 was driven by a 25 hp pump and manufactured from aluminum, dimensioned to sustain pressures of up to 0.5 MPa. To reduce the amount of vapor bubbles suspended in the flow completing the loop, the stagnation box upstream of the testsection was fitted with three fine meshes (380 μm, 104 μm and 74 μm pore size, respectively). The tunnel was equipped with Omega PX303 pressure transducers on the stagnation chamber and the collection box and an RTD for temperature monitoring on the stagnation chamber. To reduce the amount of dissolved gas, the tunnel was connected to vacuum through a dry ice-cooled recuperation coil for a few hours prior to the experiments.

B. Hydrofoils

Two c=50.8 mm chord, 102 mm span NACA0015 hydrofoils were manufactured from aluminum. One was fitted with pressure taps at the locations x/c=0.00, 0.06, 0.11, 0.17, 0.21, 0.32 and 0.88 along the suction side centerline. Each tap was connected to a 200kPa (30 psia) Omega PX303 pressure transducer using tubing that was filled with liquid fluoroketone prior to testing to ensure fast response. The second hydrofoil was fitted with a PET cover and an internal 45° mirror that allowed a laser sheet to be projected out from the hydrofoil along its centerline, as seen in Figure 1b. The 351 nm output of a Nd:YLF laser capable of producing 50 μJ/pulse at 1 kHz repetition rate was fed to the hydrofoil through an optical fiber and sheet-forming fused silica lenses. Images were taken using a PI Acton PIMAX2 intensified CCD camera or a pco.1200s high-speed camera capable of kHz-range frame rates.

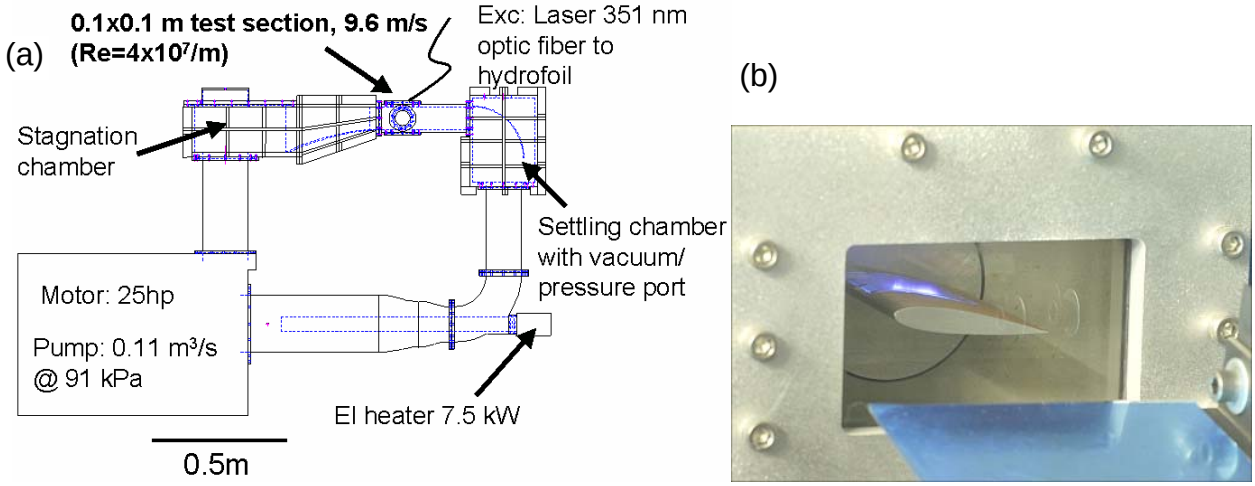

Figure 1. Sketch of the watertunnel used in the experiments (a) and photograph of front of testsection showing fluorescence produced as the UV laser sheet enters the fluorinated ketone above the hydrofoil (b).

III. Results

A. Flash Exposure Images

Images of the cavitation were taken using two discharge bulbs firing with a spacing of 4.5 ms providing acceptably even illumination over 10 ms. A sequence of images was acquired at 1270 fps at various flow speeds while simultaneously acquiring pressure data. Figure 2 shows four selected images from such a sequence illustrating the approximately periodic nature of the cavity development under these conditions. While the 7 ms periodicity seen in the images corresponds to a frequency of 140 Hz, the test section static pressure acquired during the same run featured a broad peak centered at 50 Hz as well as a narrow peak, possibly a higher harmonic, near 145 Hz, seen in Figure 3. Figure 2 also shows the small size of the bubbles (<0.1 mm) formed in the fluoroketone even under ambient conditions, in contrast to the much larger (>1 mm) bubbles seen in water under similar conditions.[8,9]

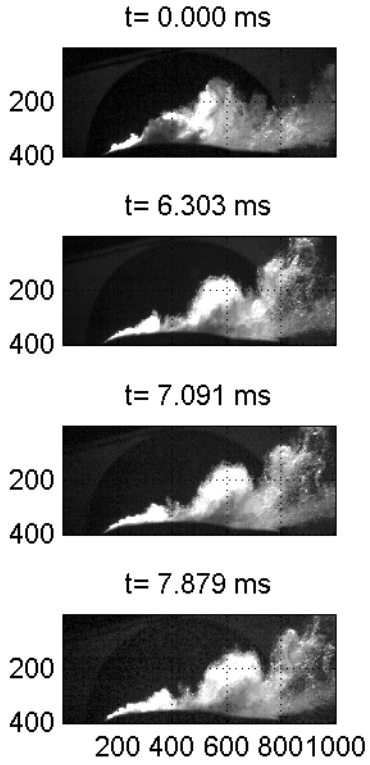

Figure 2. Four side-view images from a dual-flash exposure sequence at 5.2 m/s and α=8°, corresponding to σ=1.62 showing a rough cavitation periodicity of 7 ms. Axes indicate pixels, 1 pixel=60μm. The flash duration was not long enough to capture the potential Mode II oscillation near 50 Hz.

B. Pressure Measurements

The pressure measurements presented in Figure 3 were obtained after degassing the fluoroketone in the test facility. As Figure 3a shows, cavitation, which occurs gradually on the hydrofoil as the tunnel speed is increased, leads to a decrease in the maximum suction peak and the formation of a longer region of more moderately adverse pressure gradient. Bubble formation and a reduced suction peak are observed even before σ approaches $(-C_P)_{min}$. As indicated in Figure 3b, the change is also associated with the appearance of pressure oscillations with a peak frequency of ~50 Hz at 5.2 m/s and then at ~10 Hz for higher speeds. When the Strouhal number based on these frequencies and the chord length c=51 mm are calculated, they are found to be 0.49 at 5.2 m/s, 0.07 at 6.7 m/s and 0.10 at 8.6 m/s, respectively. Also seen in Figure 3b are the distinct blade-passing frequencies of the pump of 80 Hz at 6.7 and 100 Hz at 8.6 m/s.

As the oscillations grow increasingly strong, there is also a notable decrease in the suction peak near x/c=0.05 as shown in Figure 3. Farther downstream, the impact is smaller with a dramatic decrease in the pressure gradient

leading to larger -C_P for x/c>0.25. C_P approaches a plateau, but still exhibits some recovery going downstream, even at the lowest cavitation numbers. This is in line with observations by Tani & Nagashima[10] in the presence of strong thermodynamic effect.

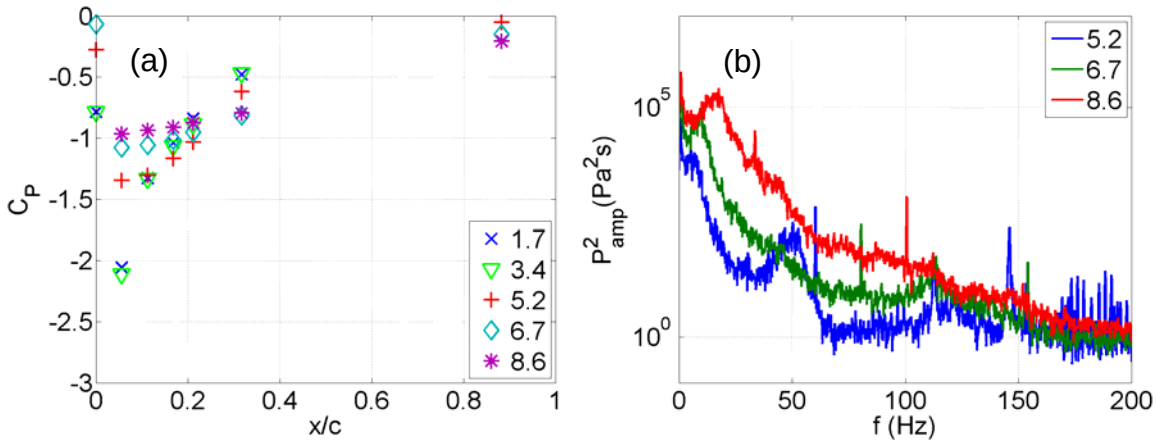

Figure 3. Pressure coefficient profiles (a) and fluctuation spectra (b) at varying speeds (m/s) at α=8°. σ=1.62 at 5.2 m/s, σ=1.15 at 6.7 m/s, and σ=1.30 at 8.6 m/s.

C. Laser-Induced Fluorescence Images

The fluorescence images show a large cavitating region covering the entire region accessible to the laser sheet, 0.3<x/c<0.6, at 7° and freestream speeds above 5 m/s. The images in Figure 4 have been corrected for spatial laser-sheet intensity variation and the contour of the hydrofoil has been overlaid in a coordinate system with the origin at the leading edge of the hydrofoil. The region with significant vapor concentration can be seen to grow from 0.13c to 0.18c over the region studied. The variation between instantaneous images is large, partly due to the varying thickness of the vapor layer in the laser sheet and partly due to different amounts of obstructing phase interfaces between the centerline and the observation window. The images illustrate the disappearance of the discrete liquid-vapor interface seen in the absence of a strong thermodynamic effect.

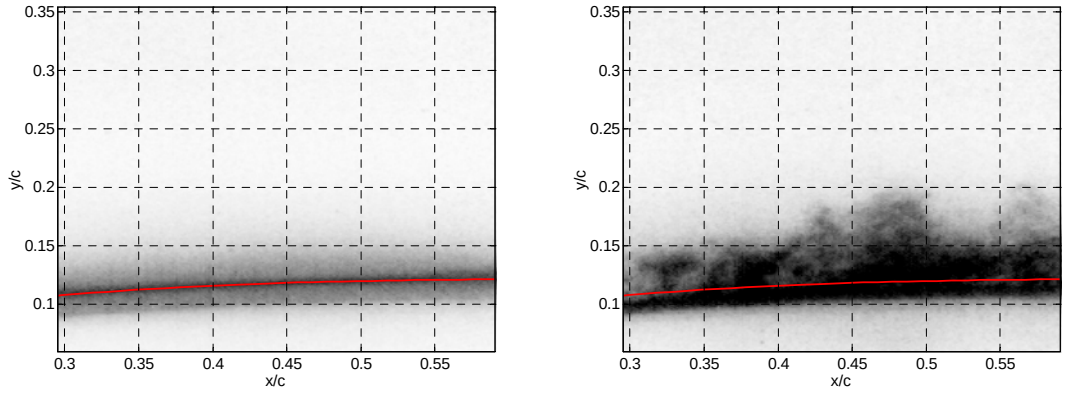

Figure 4. Instantaneous fluorescence intensity over 50 frames corrected for laser-sheet uniformity at 0 m/s (left) and 5.2 m/s (right).

IV. Discussion

It should be noted that separate tests suggested a 1/e response for the hydrofoil taps of 50 Hz, implying that the amplitude of the cavitation peaks is likely suppressed by an order of magnitude. Nevertheless, the observed peak frequencies are in only partial agreement of those observed by Kjeldsen et al[5] in water for Mode II cavitation: Rather that exhibiting an increasing St_c with increasing σ, St_c here remained constant, St_c =0.56±0.03 over a wide range of cavitation numbers, 1.3<σ<2.6 or 5.5<$\sigma/2\alpha$<10.8. A similar trend, but with very broad peaks, was seen by Sato et al[11] on a flat plate at α=5°, with the Strouhal number increasing from St_c=0.125 at $\sigma\leq$1.12 to St_c=0.43 at σ=1.25 and

St_c=0.82 at σ=1.54. Arndt et al[12] suggest a transition between type I and II cavitation at $\sigma/2\alpha$=4, with the frequency growing linearly with increasing σ: St_c =0.3($\sigma/2\alpha$ -3). This would produce fluctuations at a frequency three times higher than observed in the present tests. The broadband low-frequency noise seen in all spectra in the present study are referred to as Type III oscillations due to bubble-patch cavitation.[12] However, the appearance of the cavitation is quite different from that seen at cavitation numbers σ=2.7 at α=8°, where Arndt et al's classification scheme suggest l/c<1/3, but flash images in the present study show that bubble formation extends over the entire hydrofoil, as seen in Figure 2. This is believed to be a result of residual dissolved gas being extracted from the liquid rather than proper cavitation. In contrast, in runs carried out after degassing the fluoroketone, behavior generally consistent with the Mode I-II transition is observed in the pressure spectra with a St_c~0.15 peak developing as $\sigma/2\alpha$ is reduced below 4. Above this, a broad peak at a St_c similar to that observed for dissolved gas-related oscillations is observed. This is shown in Figure 5. Cervone et al observed a similar transition, but in contrast to the present study, their fundamental St_c=0.2 peak was visible across the whole cavitating range σ<2.1 for α=8°. When comparing the present data with that obtained in liquid nitrogen by Tani and Nagashima,[10] the gradual recovery downstream of the suction peak is observed, but in contrast to their data, the minimum pressure observed is here well above the vapor pressure, even basing it on the free-stream temperature.

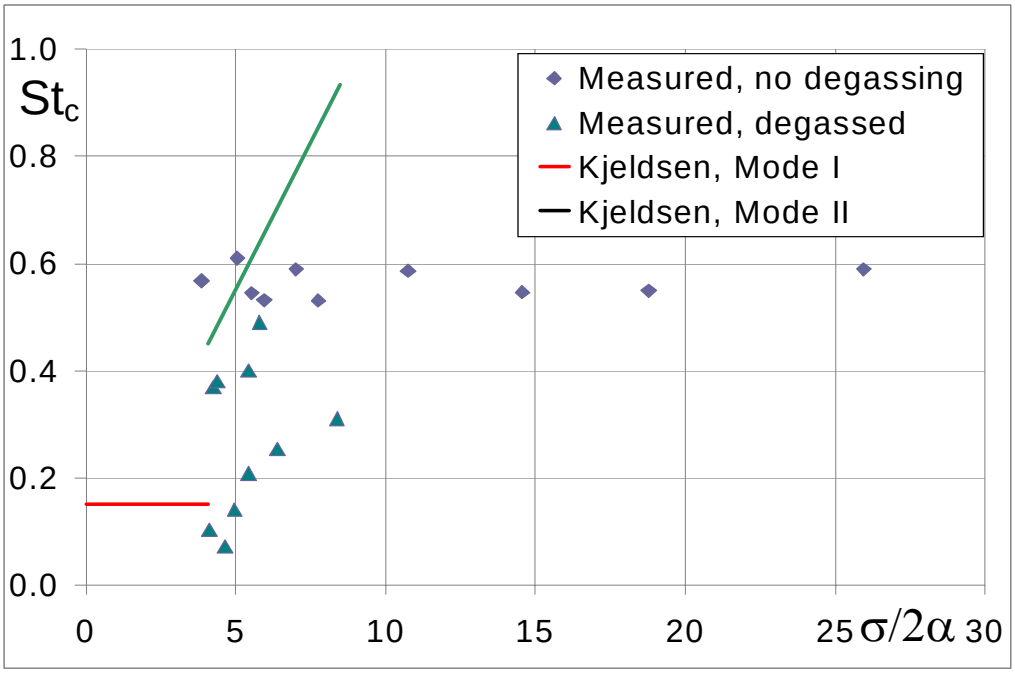

Figure 5. Chord-based Strouhal number for dominant fluctuations as a function of angle-of-attack-corrected cavitation number. Comparison to results of Kjeldsen et al.[5]

V. Conclusion

This study demonstrated that:

- The dominant frequency corresponds to a Strohaul number of 0.56 based on hydrofoil chord over a wide range of cavitation numbers, in contrast to the larger and cavitation-number-dependent Strouhal numbers seen in earlier water tests. This is believed to be due to dissolved gas coming out of solution rather than proper cavitation.
- With proper degassing, the mode I-II transition appears to occur in a similar manner to what has been observed in water with a low-frequency peak developing at $\sigma/2\alpha$<4, while St_c increases rapidly above this cavitation number.
- The cavitation in fluoroketone exhibits the finer structure expected of a fluid with stronger thermodynamic effect.

- Bubbles are formed and oscillations seen well before the pressure on the hydrofoil has dropped to the saturation vapor pressure.
- Even at cavitation numbers as low as $\sigma \approx 1.2$, the C_P curves are not perfectly flat but exhibit slight downstream recovery.

Acknowledgments

This work has been supported by a NASA Constellations grant under Program Manager Claudia Meyer. We also thank Wei Shyy and Dan Dorney for fruitful discussions.

References

[1] Franc, J-P, Rebattet, C, Coulon, A, "An experimental investigation of thermal effects in a cavitating inducer", *5th International Symposium on Cavitation (Cav2003)*, Osaka, Japan, 2003.
[2] Billet, M. L., Holl, J. W., Weir, D. S., "Correlations of Thermodynamic Effects for Developed Cavitation", *Journal of Fluids Engineering*, **103** (12), p. 534-542, 1981.
[3] Brennen, C. E., *Hydrodynamics of Pumps*, Oxford University Press, Oxford, 1994.
[4] Brennen, C. E., *Cavitation and Bubble Dynamics*, Oxford University Press, New York, 1995.
[5] Kjeldsen,M., Arndt, R. E. A., and Effertz, M., "Spectral Characterization of Sheet/Cloud Cavitation", *Journal of Fluids Engineering*, **122** (9), pp. 481-487, 2000.
[6] Bissell, W. R., Wong, G. S., Winstead, T. W., "Analysis of Two-Phase Flow in LH_2 Pumps for O_2/H_2 Rocket Engines", *Journal of Spacecraft*, **7** (6), 1970.
[7] Gustavsson, J. P. R., Segal, C., "Fluorescence spectrum of 2-trifluoromethyl-1,1,1,2,4,4,5,5,5-nonafluoro-3-pentanone", *Applied Spectroscopy*, **61** (8), 2007.
[8] Rapposelli, E., Cervone, A., Bramanti, C., d'Agostino, L., "Thermal cavitation experiments on a NACA 0015 hydrofoil", *4th ASME_JSME Joint Fluids Engineering Conference*, Honolulu, HI, 2003.
[9] Cervone, A., Bramanti, C., Rapposelli, E., d'Agostino, L., "Thermal Cavitation Experiments on a NACA 0015 Hydrofoil", *Transactions of the ASME*, **128** (3), p. 326-331, 2006
[10] Tani, N., Nagashima, T.,"Cryogenic Cavitating Flow in 2D Laval Nozzle", *Journal of Thermal Science*, **12** (2), p. 157-161, 2003
[11] Sato, K., Tanada, M., Monden, S., Tsujimoto, Y., "Observations of Oscillating Cavitation on a Flat Plate Hydrofoil", *4th International Symposium on Cavitation (Cav2001)*, Pasadena, CA, USA, 2001.
[12] Arndt, R. E. A., Balas, G. J., Wosnik, M., "Control of Cavitating Flows: A Perspective", *JSME International Journal*, Series B, **48** (2), p. 334-341, 2005.